Adsorption (2008) 14: 781–789
DOI 10.1007/s10450-007-9085-6

High temperature adsorption of CO_2 on various hydrotalcite-like compounds

Nick D. Hutson · Brian C. Attwood

Received: 29 January 2007 / Revised: 26 November 2007 / Accepted: 18 December 2007 / Published online: 5 February 2008

Abstract A study was conducted to describe and quantify how substitution of the divalent cation and interlayer charge compensating anions affect the CO_2 adsorptive capacity of various hydrotalcite-like compounds (HTlcs). Physical and chemical properties of the HTlcs were evaluated using a number of methods and the CO_2 adsorption rate and capacity were measured at elevated temperature (603 K). The results showed that the synthetic analogue of the naturally occurring hydrotalcite mineral, $[Mg_{0.73}Al_{0.27}(OH)_2](CO_3)_{0.13} \cdot xH_2O$, had the best overall adsorption capacity and kinetics. The stability of the adsorption capacity was tested by subjecting the model HTlc to 10 equilibrium adsorption and desorption cycles. At the end of the cycle, the HTlc had maintained approximately sixty-five percent of its initial capacity. Temperature programmed desorption of CO_2 was used to quantify the surface basicity of the various HTlcs. The results showed that the reversible physisorption portion of the CO_2 isotherm was correlated to the number of surface basic sites on the HTlcs.

Keywords Layered double hydroxides · LDH · Hydrotalcite · HTlc · CO_2 adsorption · Carbon capture

1 Introduction

Carbon capture and sequestration has been proposed as one option for control of carbon emissions from stationary sources. While no portion of this scheme is trivial, it is the separation and capture of the CO_2 that presents one of the biggest challenges, both technically and economically. Adsorption has been used for many years for a wide variety of gas separations (Yang 1997) and has been proposed for CO_2 separation and capture from fossil-fueled power plants and other sources (Kikkinides et al. 1993; Gomes and Yee 2002). The effectiveness of any adsorption-based separation depends greatly upon the adsorbent chosen for the application and there are a number of synthetic and naturally occurring materials with high CO_2 adsorption capacity. However, most of the commonly studied adsorbents (zeolites, activated carbons, etc.) suffer from low capacity at elevated temperatures. Several materials have been shown to have adsorptive capacity for CO_2 at the higher temperatures seen in combustion processes. These materials include CaO (Lu et al. 2006), lithium zirconate (Li_2ZrO_3)(Ida and Lin 2003), and hydrotalcite-like compounds (HTlcs) (Hutson et al. 2004).

HTlcs are bi-dimensional basic clays with a structure consisting of positively-charged brucite-like (magnesium hydroxide) layers and an interlayer space containing charge-compensating anions and water molecules (Ulibarri et al. 2001). The metal cations occupy the centers of octahedra whose vertices contain hydroxide ions and are connected by edge sharing to form an infinite sheet (Constantino and Pinnavaia 1995). The general formula of the compounds is $[M^{2+}_{1-x}\ M^{3+}_x(OH)_2]A^{n-}_{x/n}$, where M^{2+} and M^{3+} are divalent (Mg^{2+}, Zn^{2+}, Ni^{2+}, etc.) and trivalent cations (Al^{3+}, Cr^{3+}, etc.). A^{n-} is a non-framework charge-compensating anion (such as CO_3^{2-}, Cl^-, SO_4^{2-}, etc.), and x is normally between 0.17 and 0.33 (Ulibarri et al. 2001). The general structure is shown in Fig. 1.

Previously published results of CO_2 sorption on HTlcs suggest that they may be useful for CO_2 separation and capture (Ding and Alpay 2000; Yong et al. 2001; Reynolds et

N.D. Hutson (✉) · B.C. Attwood
National Risk Management Research Laboratory, Office of Research and Development, U.S. Environmental Protection Agency, 109 T. W. Alexander Drive (E305-01), Research Triangle Park, NC 27711, USA
e-mail: hutson.nick@epa.gov

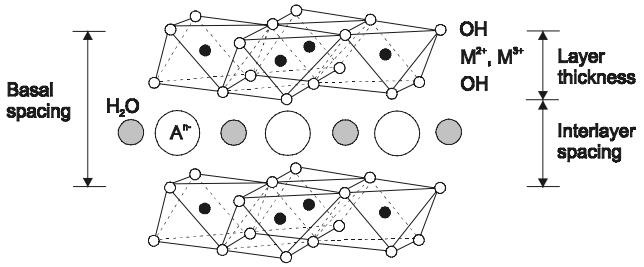

Fig. 1 Structure of hydrotalcite-like compounds. In this diagram M^{2+} and M^{3+} represent di- and tri-valent cations which, with the –OH molecules, form the layered structure of the HTlc. The interlayer spacing is occupied with charge-compensating anions (A^{n-}) and water molecules

al. 2005). HTlcs are very open to physical and chemical manipulation and numerous combinations of structural cations and interlayer charge-compensating anions have been synthesized. The structure and properties of the materials can also be modified for specific application by thermal treatment (Hutson et al. 2004). The adsorption capacity and the stability of hydrotalcite-like adsorbents have been enhanced by promotion with alkali salts (Ding and Alpay 2000; Mayorga et al. 2001) and by small additions of rare earth elements to the hydrotalcite structure (White et al. 2003). The presence of water vapor has also been shown to enhance the CO_2 capacity and slow the rate of deactivation for hydrotalcite-like sorbents (Ding and Alpay 2000). With the proper understanding of composition-structure-property relationships, HTlcs may, conceivably, be synthesized and tailored as effective high temperature sorbents for CO_2 separation and capture. In this work we have attempted to describe and quantify how substitution of the divalent cation and interlayer charge compensating anions affect the CO_2 adsorptive capacity of the HTlc.

2 Materials and methods

2.1 Synthesis

A synthetic analog of the naturally occurring hydrotalcite mineral, $[Mg_{0.75}Al_{0.25}(OH)_2](CO_3)_{0.125}\cdot mH_2O$, was prepared via a co-precipitation technique. In the synthesis procedure, 0.75 mol $Mg(NO_3)_2\cdot 6H_2O$ and 0.25 mol $Al(NO_3)_3\cdot 9H_2O$ were dissolved in 250 mL deionized (DI) water. The solution was then added, dropwise with vigorous stirring, to a 500 mL solution containing 1.7 mol NaOH and 0.5 mol Na_2CO_3. The resulting precipitate was then separated by vacuum filtration, washed with DI water and dried at 100 °C in a conventional oven. The dried solid was crushed in a mortar and pestle and stored in a glass sample bottle for subsequent characterization.

In an analogous manner, samples of the following HTlcs were prepared: $[Ca_{0.75}Al_{0.25}(OH)_2](CO_3)_{0.125}$ (the M^{2+} source was $Ca(NO_3)_2\cdot 4H_2O$), $[Mg_{0.75}Al_{0.25}(OH)_2](Cl)_{0.25}$ (the A^{n-} source was NaCl), $[Mg_{0.75}Al_{0.25}(OH)_2](ClO_4)_{0.25}$ (the A^{n-} source was $NaClO_4$), and $[Mg_{0.75}Al_{0.25}(OH)_2][Fe(CN)_6]_{0.0625}$ (the A^{n-} source was $K_4Fe(CN)_6$). For the remainder of this paper, these samples are referred to by the following shorthand notation, $(M^{2+},M^{3+})(A^{n-})$.

2.2 Surface area and porosity

The total surface area and porosity of the HTlcs were calculated from N_2 adsorption isotherms that were obtained at 77 K using a static volumetric system (Quantachrome Autosorb-1-C/MS). The isotherms were measured using samples that had been pretreated by heating in a vacuum at 573 K for a minimum of 4 hours. The surface area was calculated using the BET method. The pore volume was calculated from the adsorbed amount at $P/P_0 \approx 1$, assuming that the pores are filled with liquid adsorbate. The average pore diameter was calculated from the pore volume and surface area assuming cylindrical pore geometry. The microporosity was evaluated using the Horvath-Kawzoe (H-K) and Dubinin-Radushkevitch (D-R) equations assuming slit-type pores.

2.3 X-ray diffraction

Powdered x-ray diffraction (XRD) patterns were collected using a Siemens D-500 diffractometer using Cu Kα radiation scanning over a 2θ range of 5 to 85° in steps of 0.02°. The scans were conducted at room temperature on samples that had not been degassed or heat treated. The resulting patterns were compared to reference patterns for the naturally occurring hydrotalcite mineral. The basal spacing (see Fig. 1) was calculated with Bragg's Law using the d_{003} peak from the diffraction pattern. Crystallinity of the samples was calculated as the ratio of the area under the peaks minus the background to the total area under the signal curve.

2.4 Thermogravimetry and rate of adsorption

Thermogravimetric analysis of the samples was performed using a Perkin-Elmer TG-7 thermogravimetric analyzer (TGA). Approximately 10 mg of each sample was heated from room temperature to 823 K at 10 K/min under helium gas flowing at 50 mL/min. The weight loss was calculated as a percentage of initial weight.

Experiments to measure the rate of CO_2 adsorption by the sorbents were also done using the TG-7 TGA. For those experiments approximately 5 mg of each sample was

heated from room temperature to 673 K at 10 K/min under helium gas flowing at 50 mL/min. The sample was held at 673 K for 30 minutes, cooled to 573 K at 10 K/min, and held for 30 minutes. The gas input was then switched to dry industrial-grade CO_2 gas and held for 90 minutes. The amount of CO_2 gas adsorbed was determined from the change in mass during CO_2 flow. Effects due to the change in gas viscosity and gas density were corrected by measuring the response to a non-adsorbing blank—in this case a piece of aluminum foil. The blank response, which was very small for these experiments, was subtracted from the sample response. Though the presence of water vapor has been shown to improve the CO_2 adsorption capacity (Ding and Alpay 2000), no water vapor was added during these experiments.

2.5 Surface basicity

The surface basicity of the materials was determined using temperature programmed desorption (TPD) of CO_2. These experiments were performed using the Quantachrome Autosorb-1-C/MS. With each test, an approximate 0.3 g sample of the sorbent was loaded into a flow-through chemisorption quartz cell. The sample was then heated to 673 K at 10 K/min and held for 30 minutes under flowing helium at 100 mL/min. The sample was then cooled to 343 K and held under vacuum for one hour before being exposed, for one hour, to pure CO_2 flowing at 20 mL/min. Following this, the cell was evacuated and the sample was again held under flowing helium. A mass spectrometer (Pfeiffer Vacuum, 0–200 amu) was used to monitor the concentration of CO_2 in the helium leaving the cell. Once the concentration of CO_2 leaving the cell was stabilized, the temperature of the sample was increased from 343 K to 973 K at a rate of 10 K/min. The sample was held at 973 K and the concentration of CO_2 was allowed to return to the baseline value. The mass spectrometer was then calibrated by injecting 1 mL of CO_2 into a septum on the quartz cell.

The signal generated by the injection of 1 mL of CO_2 for calibration, minus the baseline value, was integrated with respect to time. From this, a multiplication factor for conversion of the mass spectrometer signal to volume of CO_2 could be determined for each run. The mass spectrometer signal minus the baseline value was then integrated with respect to time for the period during which the temperature was raised from 343 K to 673 K. The volume and, hence, number of moles of gas released during this period could then be calculated based on the conversion factor. Assuming a 1:1 correspondence of adsorbed CO_2 molecules to basic sites, the basic site density was then determined.

2.6 CO_2 adsorption isotherm measurements

High temperature CO_2 equilibrium adsorption isotherms were measured using the chemisorption cell of the Quantachrome Autosorb-1-C/MS. The samples were initially pretreated by heating to 673 K in vacuum. The treated sample was then cooled to 603 K and the combined (physisorption plus chemisorption) isotherm was measured. The sample was then completely evacuated (to approximately 10^{-5} Torr), at temperature, removing only the physically (weakly) adsorbed gas. The adsorption isotherm measurement was repeated to obtain the physisorption component. The chemisorption (strong) component was then determined by the difference in the combined isotherm and the physisorption (weak) isotherm. Additions of the adsorbate gas were made at volumes required to achieve a targeted set of pressures. A minimum equilibrium interval of 20 minutes with a tolerance of 0.5% for $P > 1$ Torr and 1.7% for $P < 1$ Torr was used to determine equilibrium for each measured point (i.e., the equilibrium criteria was checked every 20 minutes).

One sorbent, $(Mg,Al)(CO_3)$, was chosen to measure the stability of its CO_2 adsorption capacity over repeated adsorption/desorption cycles. The sample was initially heat treated in vacuum at 673 K for 12 hours before the measurement of the first adsorption isotherm. After that, the sample was subjected to equilibrium adsorption/desorption cycles at 573 K with no additional heating.

3 Results and discussion

3.1 Physiochemical characterization

Table 1 gives the physiochemical properties of the sorbents used in this study. There is a broad range of total surface areas for the heat-treated materials, with $(Mg,Al)[Fe(CN)_6]$ having the highest total surface area at 270.3 m^2/g and $(Ca,Al)(CO_3)$ and $(Mg,Al)(ClO_4)$ having the lowest at 21.8 m^2/g and 26.1 m^2/g respectively. The low surface area of the two latter samples is apparently due to very low microporosity, as evidenced by the large average pore diameters and the very low micropore volumes (see Table 1). Interestingly the $(Ca,Al)(CO_3)$ sample had the largest total pore volume and the largest average pore diameter of all of the samples, indicating a very open structure with limited microporosity. The $(Mg,Al)(CO_3)$, $(Mg,Al)[Fe(CN)_6]$ and (Mg,Al)(Cl) samples all had very similar physiochemical properties.

The basal spacings, d_{003} (see Fig. 1), of the various HTlc structures are similar, falling in the range of 7.6–8.0 Å, with the exception of the $(Mg,Al)(ClO_4)$ sample which had a basal spacing of 9.5 Å. The basal spacings were calculated

Table 1 Sorbent physiochemical properties

Sorbent	Surface area (BET) (m^2/g)	Pore volume (mL/g)	Average pore diam. (Å)	DR micropore volume (mL/g)	HK pore width (mode) (Å)	Basal spacing d_{003}* (Å)	Crystallinity* (%)
(Mg,Al)(CO_3)	177.4	0.325	73.4	0.094	4.4	7.74	37.2
(Mg,Al)[Fe($CN)_6$]	270.3	0.259	38.3	0.073	5.4	7.70	23.1
(Mg,Al)(Cl)	221.1	0.268	48.6	0.089	4.4	7.98	37.1
(Ca,Al)(CO_3)	21.8	0.479	877.8	0.010	4.9	7.62	54.5
(Mg,Al)(ClO_4)	26.1	0.187	286.9	0.006	16.3	9.50	59.2

*At room temperature; all other properties are after heating in vacuum at 573 K

from XRD patterns that were collected at room temperature using materials that had not been heat treated (beyond drying at 373 K). Hutson et al. (2004) examined the effects of temperature on the structure of (Mg,Al)(CO_3) and found that the basal spacing decreased from 7.8 to 7.2 Å when heated from room temperature to 473 K as the loosely held water is lost from the interlayer space. As the sample was heated from 473 to 573 K, partial decarbonation of the HTlc occurred and the basal spacing further decreased to 7.1 Å. Above 583 K, the layered structure collapsed and the material became x-ray amorphous.

Figure 2 shows the TGA profiles of the HTlc samples. The curves for the (Mg,Al)(CO_3), (Mg,Al)(Cl), and (Mg,Al)[Fe($CN)_6$] samples are all fairly similar in shape with two distinct regions of weight loss. With all three samples, there is an initial decrease in weight of approximately 15% in the temperature range of 300–450 K. This is almost entirely due to loss of loosely held water in the interlayer space and some initial decarbonation (Hutson et al. 2004). The samples then show another decrease in weight in the temperature range of 500–700 K. For the (Mg,Al)(CO_3), this is due to significant decarbonation through the loss of the interlayer charge compensating carbonate anion (as evolved CO_2) and dehydroxylation of the octahedral layers. For the (Mg,Al)(Cl) and (Mg,Al)[Fe($CN)_6$] samples, this second region of weight loss likely involves decomposition of the charge compensating anion and dehydroxylation of the octahedral layers. All of these samples end with a total weight loss of ~ 40%.

While similar in shape to those found in Fig. 2(a), the curve for (Ca,Al)(CO_3) ends in a much lower percent weight loss, 15%, than those curves. The weight loss curve for the (Mg,Al)(ClO_4) sample also showed two distinct regions. However, this sample exhibited very sharp decreases in mass in the two regions. The initial loss of almost 10% in the region 300 – 350 K is likely from loosely-held water. The weight of the sample is fairly constant until approximately 500 K, where there is another rapid weight loss. The total weight loss of the sample was approximately 42%.

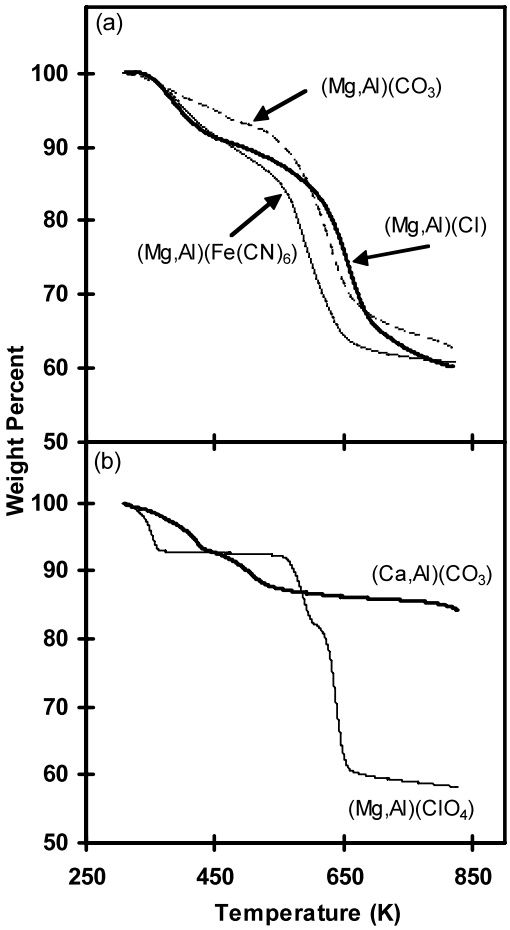

Fig. 2 TGA profiles of (**a**) (Mg,Al)(CO_3) HTlc, (Mg,Al)[Fe($CN)_6$] HTlc, and (Mg,Al)(Cl) HTlc and (**b**) (Ca,Al)(CO_3) HTlc and (Mg,Al)(ClO_4) HTlc under flowing He

Figure 3 shows a graph of the TPD profiles of the five HTlc samples. The mass spectrometer signals have been scaled based on the size of the sample and are stacked for ease of comparison. The calculated number of basic sites and the temperature at which peak desorption occurred are given in Table 2. For the (Mg,Al)(CO_3) material, the peak

Table 2 Basic site densities and peak desorption temperatures measured by TPD

Sorbent	Basic site density (μmol/g)	Basic site density (μmol/m^2)	Desorption peak (K)
(Mg,Al)(CO_3)	692	3.90	427
(Mg,Al)[$Fe(CN)_6$]	355	1.31	426
(Mg,Al)(Cl)	117	0.53	506
(Ca,Al)(CO_3)	6	0.28	408
(Mg,Al)(ClO_4)	2	0.08	413

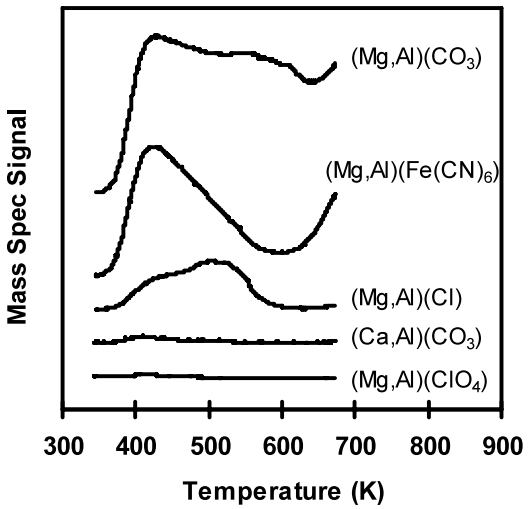

Fig. 3 Temperature programmed desorption profiles measured from 343 to 673 K at a linear heating rate of 10 K/min

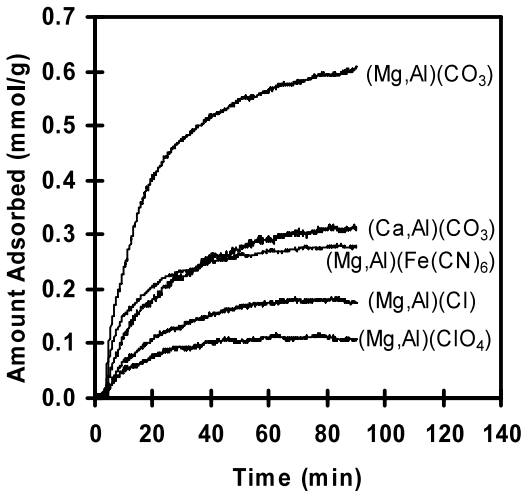

Fig. 4 Adsorption of pure CO_2 flowing at 50 mL/min at 573 K on HTlc samples degassed at 673 K in flowing helium

desorption occurs around 427 K with a second peak or shoulder at approximately 558 K indicating the presence of two types of basic sites of increasing strength. This result is in agreement with model proposed by Ebner et al. (2006) for CO_2 adsorption onto K-promoted HTlc involving multiple adsorption sites with varying strength. This material also has the highest basic site density, at 692 μmol/g, of the five HTlcs studied. The (Mg,Al)[$Fe(CN)_6$] sample had a somewhat lower basic site density of 355 μmol/g and appears to exhibit just one type of basic site, corresponding to the weaker of the two found for the (Mg,Al)(CO_3). The (Mg,Al)(Cl) was found to have a basic site density of 117 μmol/g and the desorption curve indicated the presence of two types of basic sites, the weak basic site indicated by a peak at 423 K and a second, intermediate strength basic site that yielded a peak at 506 K. The (Ca,Al)(CO_3) and (Mg,Al)(ClO_4) samples showed a very low number of weak basic sites.

3.2 CO_2 adsorption measurements

Figure 4 shows the results of the rate of adsorption experiments. The amount of CO_2 adsorbed (mmol of CO_2 per gram of sorbent) is shown to an elapsed time of 90 minutes. The (Mg,Al)(CO_3) sample shows the highest initial rate of adsorption and the highest amount of CO_2 adsorption, 0.62 mmol/g, at the end of time interval. The (Mg,Al)[$Fe(CN)_6$] has an initial rate of adsorption close to that of the (Mg,Al)(CO_3), but at the end of the experiment has a lower total amount of adsorption than the (Ca,Al)(CO_3). The (Mg,Al)(ClO_4) has the lowest rate of adsorption and total amount adsorbed, 0.11 mmol/g, despite having the largest interlayer spacing and second largest average pore diameter.

Figures 5 and 6 show the CO_2 equilibrium adsorption isotherms at 603 K for the five HTlc samples. Table 3 lists the combined CO_2 adsorption capacity of each sample at the maximum pressure, 108 kPa, the ratio of the physisorbed-to-chemisorbed CO_2 at that pressure, and the average time it took for the instrument to equilibrate at each point while generating the combined isotherms. The (Mg,Al)(CO_3), (Mg,Al)[$Fe(CN)_6$] and (Mg,Al)(Cl) equilibrium adsorption isotherms, shown in Fig. 5, all have a similar aspect. The combined isotherms for all three materials show a sharp increase in adsorption capacity at low CO_2 pressure which then becomes linear with increasing CO_2 concentration. The adsorption behavior in the low pressure region indicates the presence of

Table 3 Sorbent CO_2 equilibrium adsorption capacities (603 K)

Sorbent	Pretreatment temperature (K)	CO_2 capacity at $P/P_0 = 1$ (mmol/g)	Physisorption/chemisorption ratio at $P/P_0 = 1$	Avg time to equilibrium (min)
$(Mg,Al)(CO_3)$	673	2.29	6.89	64
$(Mg,Al)[Fe(CN)_6]$	673	0.75	5.53	75
(Mg,Al)(Cl)	673	0.44	8.95	44
$(Ca,Al)(CO_3)$	673	1.79	0.25	138
$(Ca,Al)(CO_3)$	773	0.90	0.60	–
$(Mg,Al)(ClO_4)$	673	3.55	0.15	229
$(Mg,Al)(ClO_4)$	773	1.03	0.60	–

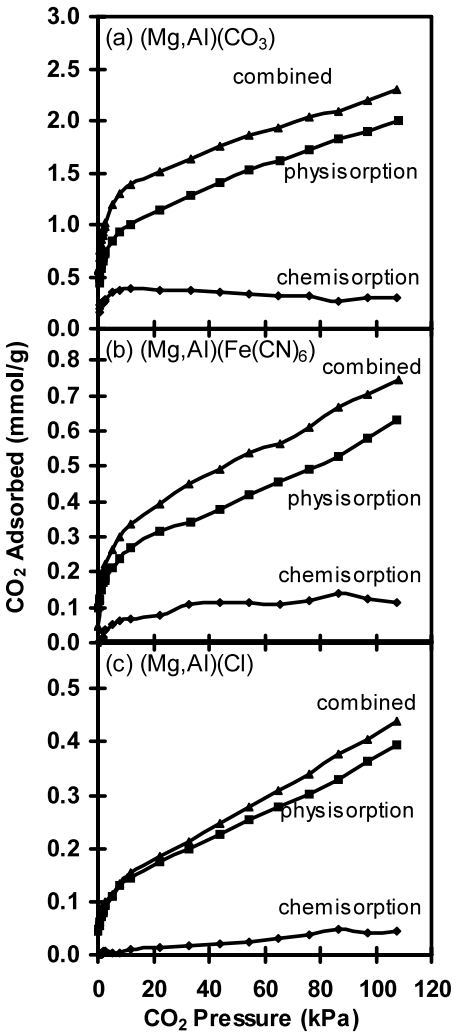

Fig. 5 CO_2 equilibrium adsorption isotherms at 603 K for (**a**) $(Mg,Al)(CO_3)$ HTlc, (**b**) $(Mg,Al)[Fe(CN)_6]$ HTlc, and (**c**) (Mg,Al)(Cl) HTlc after degassing at 673 K

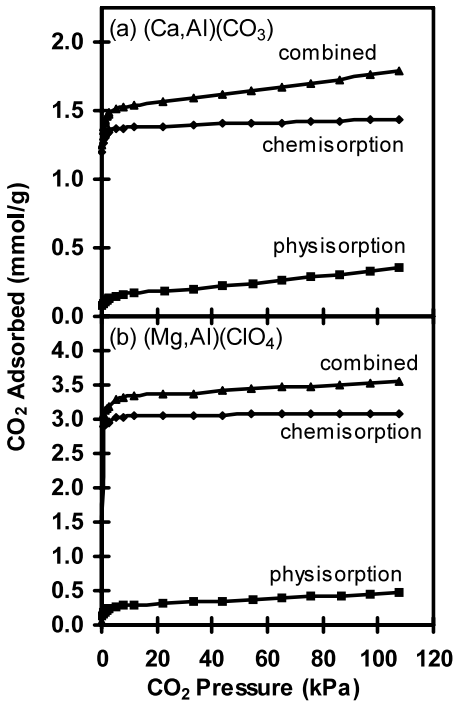

Fig. 6 CO_2 equilibrium adsorption isotherms at 603 K for (**a**) $(Ca,Al)(CO_3)$ HTlc and (**b**) $(Mg,Al)(ClO_4)$ HTlc after degassing at 673 K

strong adsorption sites, a portion of which are attributed to chemisorption sites, though the majority appear to be physisorption sites (see Fig. 5). The linear region (P_{CO_2} > 20 kPa) is almost exclusively attributable to physisorption of CO_2 to the HTlc samples. This portion of the curve represents the working capacity of the sorbent applicable to regenerative adsorptive processes such as VSA or PSA. The $(Mg,Al)(CO_3)$ sample has a combined adsorption capacity of 2.29 mmol/g at the highest pressure, 108 kPa, with 2.00 mmol/g (nearly 90%) of that capacity attributed to physisorption. The $(Mg,Al)[Fe(CN)_6]$ and (Mg,Al)(Cl) isotherms showed lower combined capacities of 0.75 mmol/g and 0.44 mmol/g at 108 kPa, respectively. The (Mg,Al)(Cl) sample did, however, have the highest ratio of physisorption-to-chemisorption and the shortest average time to equilibrium of all the HTlc samples. Table 4 com-

Table 4 Comparison of adsorption capacities for various high temperature CO_2 sorbents

Sorbent	CO_2 capacity mmol/g (@ 100 kPa)	Temp (K)	Comments	Reference
HTlc, $Ca_{0.75}Al_{0.25}(OH)_2(CO_3)_{0.125}$	1.79	603	pre-treated at 673 K; static measurement	this work
HTlc, $Ca_{0.75}Al_{0.25}(OH)_2(ClO_4)_{0.25}$	3.55	603	pre-treated at 673 K; static measurement	this work
HTlc, $Mg_{0.75}Al_{0.25}(OH)_2(CO_3)_{0.125}$	2.29	603	pre-treated at 673 K; static measurement	this work; Hutson et al. (2004)
HTlc, $Mg_{0.75}Al_{0.25}(OH)_2(CO_3)_{0.125}$	0.60	573	pre-treated at 673 K; gravimetric measurement	this work
HTlc, $Mg_{0.75}Al_{0.25}(OH)_2(CO_3)_{0.125}$	0.486	473	pre-treated at 673 K; static measurement	Reddy et al. (2006)
HTlc, $Mg_{0.75}Al_{0.25}(OH)_2(CO_3)_{0.125}$	0.249	573	pre-treated at 673 K; static measurement	Reddy et al. (2006)
HTlc*, $Mg_{0.7}Al_{0.3}(OH)_2(CO_3)_{0.15}$	0.50	573	pre-treated at 573 K; gravimetric measurement	Yong et al. (2001)
Perovskite-type metal oxides, $La_{0.1}Sr_{0.9}Fe_{0.5}O_{2.6}$	2.95	1073	sintered at 1173 K; gravimetric measurement	Yang and Lin (2006)
Lithium zirconate, Li_2ZrO_3	4.55	773	gravimetric measurement	Ida and Lin (2003)
Lithium silicate, Li_4SiO_4	6.80	873	gravimetric measurement	Venegas et al. (2007)
Calcium oxide, CaO	2.95	873	gravimetric measurement	Reddy and Smirniotis (2004)
Cs-doped CaO	11.36	873	20% Cs added; gravimetric measurement	Reddy and Smirniotis (2004)

*Sud-Chemie EXM701

pares the capacity of the sorbents studied in this work with published results for other high temperature CO_2 sorbents.

The combined equilibrium adsorption isotherms for the (Ca,Al)(CO_3) and (Mg,Al)(ClO_4) samples, shown in Fig. 6, also have a very sharp increase in capacity at very low CO_2 pressures. However, in contrast to the previously discussed samples, this low pressure behavior is almost entirely attributed to irreversible chemisorption (see Fig. 6). These samples also have the longest average times to equilibrium (at 138 and 229 min respectively).

The (Ca,Al)(CO_3) sample has a total capacity of 1.79 mmol/g at 108 kPa while that for the (Mg,Al)(ClO_4) sample was 3.55 mmol/g the highest capacity of all those measured. This is in sharp contrast to the poor performance of this material in the rate of adsorption experiment. The equilibrium adsorption isotherms for the (Ca,Al)(CO_3) and (Mg,Al)(ClO_4) samples were also measured after heat treatment at 773 K to see the effect on the CO_2 adsorption capacity. After degassing at the higher temperature, the total surface area of the two materials decreased, (Ca,Al)(CO_3) to 12.0 m^2/g and (Mg,Al)(ClO_4) to 12.5 m^2/g. The resulting CO_2 isotherms (at 603 K), shown in Fig. 7, indicate that for both samples, though there was only a slight decrease in the surface area of the samples, there was a marked decrease in the CO_2 adsorption capacity. The (Ca,Al)(CO_3) capacity at 108 kPa decreased by 50% to 0.90 mmol/g, while that of the (Mg,Al)(ClO_4) decreased by approximately 70% to 1.03 mmol/g. In both cases, the decreases in capacity were mostly due to a decrease in the chemisorption capacity.

The physisorption and chemisorption capacities (at 603 K and 108 kPa) were plotted versus the basic site density for the five HTlc samples and are shown in Fig. 8. The plots show a clear correlation of physisorption capacity with the number of basic sites on the sorbent. This suggests that the dominant means of physical adsorption involves interaction of CO_2 with basic sites created with the decomposition of the HTlc structure. There appears to be no relationship between the surface basicity and the chemisorption capacity. The irreversible chemisorption appears to be a carbonation/mineralization of the M^{2+} cations.

Consideration of the physiochemical data in Table 1 in light of the TGA curves in Fig. 2 gives some insight into the structure of each of the sorbents. The (Ca,Al)(CO_3) and (Mg,Al)(ClO_4) samples both show much lower surface areas and quantitatively different TGA curves than the other samples. In the case of the (Ca,Al)(CO_3), the XRD pattern

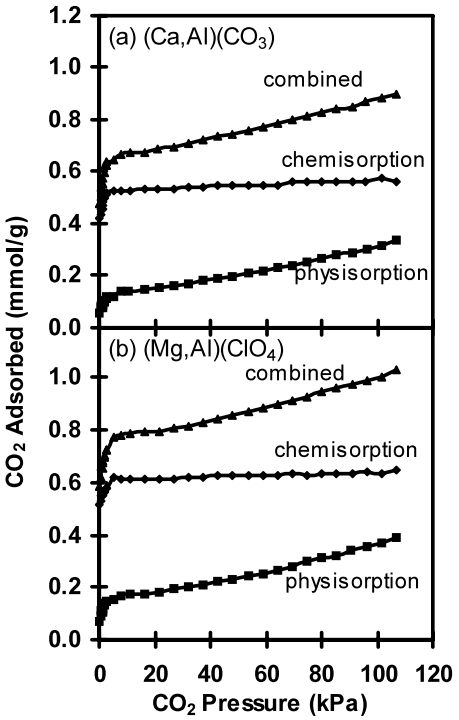

Fig. 7 CO_2 equilibrium adsorption isotherms at 603 K for (**a**) (Ca,Al)(CO_3)HTlc and (**b**) (Mg,Al)(ClO_4) HTlc after degassing at 773 K

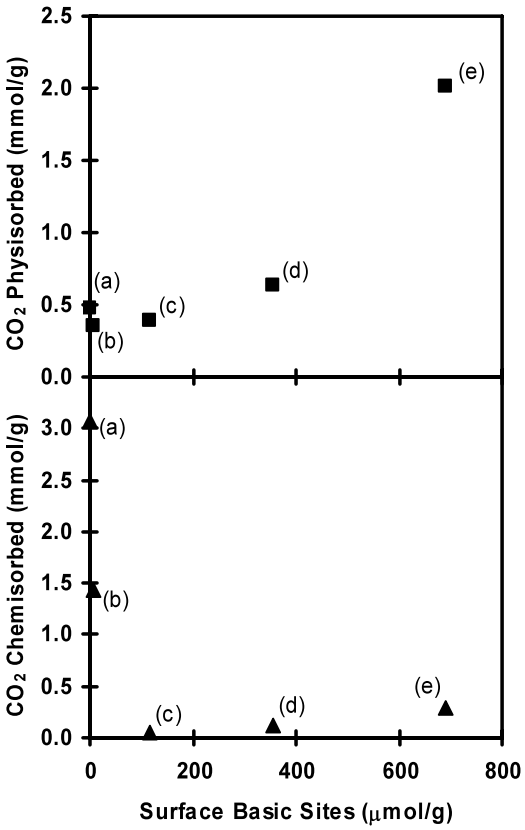

Fig. 8 The amount of CO_2 physisorbed (■) and chemisorbed (▲) vs. number of basic sites for (*a*) (Mg,Al)(ClO_4) HTlc, (*b*) (Ca,Al)(CO_3) HTlc, (*c*) (Mg,Al)(Cl) HTlc, (*d*) (Mg,Al)[$Fe(CN)_6$] HTlc, and (*e*) (Mg,Al)(CO_3) HTlc

indicated the presence of a calcite ($CaCO_3$) phase in addition to the HTlc, which may explain the lower surface area and weight loss. The XRD pattern for the (Mg,Al)(ClO_4) did not indicate the presence of a second phase, but it is possible that the bulkiness of the perchlorate ion compared to carbonate ion, while increasing the interlayer spacing of the HTlc compared to carbonate, occupied more space between the hydroxide layers resulting in less pore volume and surface area. The (Mg,Al)(CO_3), (Mg,Al)[$Fe(CN)_6$], and (Mg,Al)(Cl) had fairly similar physical properties, but significantly varying CO_2 adsorption capacities, indicating that the identity of the charge compensating anion plays a key role in determining the surface basicity of the calcined material and thus, on the affinity for CO_2 physisorption.

The rate of adsorption data presented in Fig. 4 reveals important information regarding the kinetics of CO_2 adsorption on HTlcs. At the end of the 90 minute period, it appears that the (Mg,Al)(CO_3) sample is still adsorbing CO_2, while the other sorbents seem to have reached equilibrium. For the most part, the sorbents with the highest apparent equilibrium adsorption also had the highest initial rate of adsorption, with the exception of (Mg,Al)[$Fe(CN)_6$]. The poor performance of the (Mg,Al)(ClO_4) in the rate of adsorption experiment is surprising given the high adsorption capacity exhibited by that sorbent as shown in Fig. 6. Even though the (Mg,Al)(ClO_4) appeared to have reached equilibrium at the end of the 90 minutes, it is possible that adsorption was still proceeding at a much slower pace. During the measurement of the adsorption isotherms on the Autosorb-1-C/MS, the (Mg,Al)(ClO_4) was found to have the longest run time which indicates that it likely has the slowest adsorption kinetics.

There seems to be a significant relationship between the density of basic sites and the physisorption capacity as illustrated by Fig. 8. While there appears to be a high correlation between the surface area of the HTlcs and their respective basic site densities it can be seen in Table 3 that those samples with low surface areas, (Mg,Al)(ClO_4) and (Ca,Al)(CO_3), still under-perform on a per square meter of surface area basis. Furthermore, despite their low surface areas, these two samples still have high combined adsorption capacities compared to the other samples. This result points to differences in the chemistry of the exposed surface area of the HTlcs playing a large role in determining the physisorption capacity rather than just the availability of surface area.

The stability of the (Mg,Al)(CO_3) over ten adsorption/desorption cycles is shown in Fig. 9. The plot shows an initial sharp drop in capacity due to the occupation of irreversible chemisorption sites. The capacity then continues to

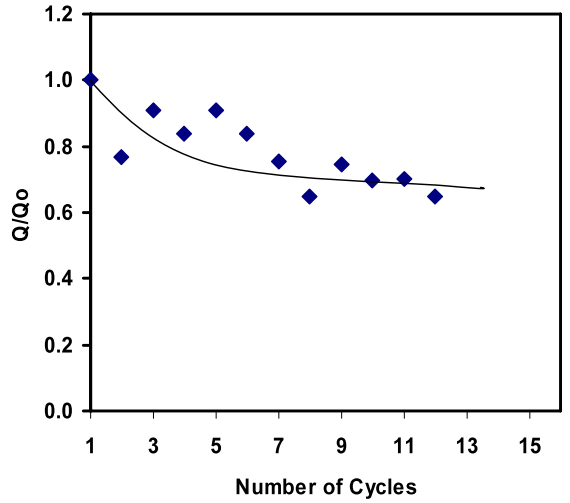

Fig. 9 Physisorption capacity of CO_2 on (Mg,Al)(CO_3) HTlc at 573 K over ten adsorption/desorption cycles

drop for a few cycles before leveling off at about two-thirds of that of the starting capacity.

Acknowledgements Much of this work was performed at the U.S. EPA and supported, in part, by the appointment of Brian Attwood to the Postdoctoral Research Program at the National Risk Management Research Laboratory, administered by the Oak Ridge Institute for Science and Education (ORISE) through an Interagency Agreement BW89938167 between the U.S. Department of Energy (DOE) and the U.S. EPA. Mention of trade names of commercial products and companies does not constitute endorsement or recommendation for use.

References

Constantino, V.R.L., Pinnavaia, T.J.: Basic properties of $Mg^{2+}_{1-x}Al^{3+}_x$ layered double hydroxides intercalated by carbonate, hydroxide, chloride, and sulfate anions. Inorg. Chem. **34**, 883–892 (1995)

Ding, Y., Alpay, E.: Equilibria and kinetics of CO_2 adsorption on hydrotalcite adsorbent. Chem. Eng. Sci. **55**, 3461–3474 (2000)

Ebner, A.D., Reynolds, S.P., Ritter, J.A.: Understanding the adsorption and desorption behavior of CO_2 on a K-promoted hydrotalcite-like compound (HTlc) through nonequilibrium dynamic isotherms. Ind. Eng. Chem. Res. **45**, 6387–6392 (2006)

Gomes, V.G., Yee, K.W.K.: Pressure swing adsorption for carbon dioxide sequestration from exhaust gases. Sep. Purif. Technol. **28**, 161–171 (2002)

Hutson, N.D., Speakman, S.A., Payzant, E.A.: Structural effects on the high temperature adsorption of CO_2 on a synthetic hydrotalcite. Chem. Mater. **16**, 4135–4143 (2004)

Ida, J., Lin, Y.S.: Mechanism of high-temperature CO_2 sorption on lithium zirconate. Environ. Sci. Technol. **37**, 1999–2004 (2003)

Kikkinides, E.S., Yang, R.T., Cho, S.H.: Concentration and recovery of CO_2 from flue gas by pressure swing adsorption. Ind. Eng. Chem. Res. **32**, 2714–2720 (1993)

Lu, H., Reddy, E.P., Smirniotis, P.G.: Calcium oxide based sorbents for capture of carbon dioxide at high temperatures. Ind. Eng. Chem. Res. **45**, 3944–3949 (2006)

Mayorga, S.G., Weigel, S.J., Gaffney, T.R., Brzozowski, J.R.: US Patent No. 6,280,503 B1, 28 August 2001

Reddy, E.P., Smirniotis, P.G.: High-temperature sorbents for CO_2 made of alkali metals doped on CaO supports. J. Phys. Chem. B **108**, 7794–7800 (2004)

Reddy, M.K.R., Xu, Z.P., Lu, G.Q., Diniz da Costa, J.C.: Layered double hydroxides for CO_2 capture: structure evolution and regeneration. Ind. Eng. Chem. Res. **45**, 7504–7509 (2006)

Reynolds, S.P., Ebner, A.D., Ritter, J.A.: New pressure swing adsorption cycles for carbon dioxide sequestration. Adsorption **11**, 531–536 (2005)

Ulibarri, M.A., Pavlovic, I., Barriga, C., Hermosin, M.C., Cornejo, J.: Adsorption of anionic species on hydrotalcite-like compounds: effect of interlayer anion and crystallinity. Appl. Clay Sci. **18**, 17–27 (2001)

Venegas, M.J., Fregoso-Israel, E., Escamilla, R., Pfeiffer, H.: Kinetic and reaction mechanism of CO_2 sorption on Li_4SiO_4: study of the particle size effect. Ind. Eng. Chem. Res. **46**, 2407–2412 (2007)

White, M.G., Iretskii, A.V., Weigel, J.S., Chiang, R.L., Brzozowski, J.R.: International Patent No. WO2004/000440 A1, 31 December 2003

Yang, Q., Lin, Y.S.: Kinetics of carbon dioxide sorption on perovskite-type metal oxides. Ind. Eng. Chem. Res. **45**, 6302–6310 (2006)

Yang, R.T.: Gas Separation by Adsorption Processes. Imperial College Press, London (1997)

Yong, Z., Mata, V., Rodrigues, A.E.: Adsorption of carbon dioxide onto hydrotalcite-like compounds (HTlcs) at high temperatures. Ind. Eng. Chem. Res. **40**, 204–209 (2001)